Eur. Phys. J. A **7**, 59–64 (2000)

THE EUROPEAN PHYSICAL JOURNAL A

EDP Sciences

Fission fragment anisotropies for ^{19}F + ^{209}Bi system

A.M. Samant[2], S. Kailas[1], A. Chatterjee[1], A. Shrivastava[1], A. Navin[3], P. Singh[1]

[1] Nuclear Physics Division, Bhabha Atomic Research Centre, Bombay 400 085, India
[2] I.N.F.N and Department of Physics, University of Padova, 35131, Padova, Italy
[3] NSCL, Michigan State University, East Lansing, USA

Received: 5 May 1999 / Revised version: 25 July 1999
Communicated by C. Signorini

Abstract. The fission fragment angular distributions have been measured for the system ^{19}F + ^{209}Bi over a range of bombarding energies from 88.0 MeV to 125.6 MeV. The measured fission fragment anisotropies are in agreement with the saddle point statistical model calculations in the above energy range. Combining these data with those available for ^{11}B, ^{12}C, ^{14}N, ^{16}O and ^{18}O + ^{209}Bi, ^{208}Pb systems, it is concluded that the spherical target plus projectile systems behave 'normal' from near- to above – barrier energies. This observation is in contrast to the 'anomalous' anisotropies exhibited by the deformed actinide target – projectile systems at near – barrier energies.

PACS. 25.70.Jj Fusion and fusion-fission reactions

1 Introduction

In recent years, the study of heavy-ion induced fission fragment angular distributions has brought out many interesting features of fission phenomena in general and fission dynamics in particular. The measured fission fragment anisotropies are found to depend on the bombarding energy relative to the fusion barrier, entrance channel of the colliding nuclei, shape, size and spin of the projectile and/or target and compound nuclear shell closure [1,2,3,4]. At above fusion barrier energies, the role of the entrance channel in influencing the measured anisotropies has been reported in fission measurements for ^{6,7}Li,^{10,11}B, ^{12}C, ^{16}O and ^{19}F + ^{232}Th, ^{238}U systems [1]. While the fission fragment anisotropies are well accounted for by saddle point statistical model (SPSM) for lighter projectiles (B, C) having entrance channel mass asymmetry α larger than α_{BG} (Businaro–Gallone critical value) but are larger than the SPSM calculations for the heavier projectiles (O, F) having $\alpha < \alpha_{BG}$. This kind of entrance channel dependence is interpreted to be arising due to the presence of fission like events from pre-equilibrium (PEQ) fission [5] in addition to compound nucleus fission. The PEQ fission is expected only in the case of the heavier of the above projectiles, on the basis of the variation of the driving force at the saddle in the mass asymmetry degree of freedom calculated as per liquid drop model. The above study, however, involved formation of different compound nuclei and hence a definitive test of entrance channel mechanism requires populating the same composite system at the same excitation energy and if possible,even with similar angular momenta. With this motivation, fission data have been measured [3] for three entrance channels that lead to the same compound nucleus, ^{248}Cf. Two of these entrance channels, ^{11}B + ^{237}Np ($\alpha = 0.911$) and ^{12}C + ^{236}U ($\alpha = 0.903$) have α greater than $\alpha_{BG} = 0.9$ and the third system ^{16}O + ^{232}Th ($\alpha = 0.871$) has $\alpha < \alpha_{BG}$. It is observed that although the anisotropy values differ at lower excitation energies (E_x = 45 to 60 MeV) and bombarding energies up to 20% above the barrier for the three systems, this entrance channel dependence is washed out at higher E_x.

However, at near-barrier and sub-barrier energies, many systems with deformed actinide targets exhibited anomalous anisotropies, irrespective of the entrance channel [1]. Several plausible reasons have been proposed to explain this [6]. At these low energies, it was recently shown [2] that even for the deformed targets, if the target spin effects (J >0) are included in the calculation, then the measured fission anisotropy data could be explained by theory. In contrast, the fission anisotropies measured for spherical targets plus projectile systems, ^{11}B, ^{12}C, ^{14}N, ^{16}O + ^{209}Bi, ^{16}O + ^{208}Pb were found to be nearly 'normal', consistent with the SPSM calculations at near- and above-barrier energies [7,8,9]. It is of interest to extend these investigations with ^{19}F as projectile on ^{208}Pb and ^{209}Bi targets as these systems have entrance channel mass asymmetry values smaller than for systems studied before and hence conditions will be more favourable to look for possible presence of entrance channel dependent effects as discussed above for deformed actinide targets. As per PEQ model, if the B_f/T value (B_f is the fission barrier) of the compound nucleus is large (very much greater than one), the PEQ fraction is expected to be small even

though the system may have favourable entrance channel mass asymmetry($\alpha < \alpha_{BG}$).The observation of normal anisotropies for the spherical target plus projectile systems having large B_f/T values, at near-barrier energies is consistent with the above expectations. At higher bombarding energies, as the B_f/T values decrease and approach values close to one, the conditions will be once again favourable for the occurrence of PEQ fission in significant proportion.

Hence measurement of data at energies well above the fusion barrier for ^{19}F plus ^{209}Bi, ^{208}Pb systems is essential to verify these aspects.

Fission data spanning a range of energies already exist for ^{19}F + ^{208}Pb system [10,11]. Zhang *et al* [10] have shown that while at above barrier energies the measured anisotropies are in agreement with the SPSM, at energies near and below the barrier the values are higher than the theoretical calculations, implying anomalous behaviour at low energies. Some recent re-measurements for this system [12], indicate that the anisotropy values are lower than those measured by Zhang *et al* [10] at near-barrier energies and are in fact in good accord with the predictions of SPSM.

In the present work, the measurements have been extended to ^{19}F + ^{209}Bi system, employing a spherical target with large g.s. spin ($J = 9/2$) and having an entrance channel mass asymmetry comaparable to ^{19}F + ^{208}Pb system, to study the influence of the variables- $E_{c.m.}/V_B$, α, target spin and B_f/T -on the measured anisotropies. The measurements have been carried out over a large range of bombarding energies, $0.95 < E_{c.m.}/V_B < 1.35$ to investigate all the above mentioned aspects. A comprehensive analysis of the data in terms of SPSM has been performed taking into account the emission of pre-saddle neutrons, finite range effects in B_f, l dependence of B_f, E_R (rotational energy)and I_{eff} (effective moment of inertia) and coupled-channels effects in the determination of the compound nuclear spin distribution especially at near-barrier energies. Based on the above analysis, stringent limits have been put on the contribution of PEQ events at the highest energy investigated.

2 Experimental details and results

Experiments were performed using the 14UD BARC-TIFR Pelletron accelerator at Mumbai. The data at the highest energy was measured using the 16UD Pelletron accelerator at Nuclear Science Centre, Delhi. The measurements were carried out using self-supporting ^{209}Bi targets (thickness $\sim$ 250 μg/cm^2) and ^{19}F beam in the energy range 88.0 to 125.6 MeV. The fission fragment angular distributions were measured in the angular range of 80^0 to 170^0, from sub-barrier to well above the fusion barrier energies. Three ΔE-E silicon surface barrier telescopes and one ΔE_{gas} common to three silicon surface barrier E detectors were used to detect the fission fragments.The data were collected as two dimensional spectra for each of the six telescopes deriving the trigger signals from the ΔE detectors(thickness 11-17 μm) in the case of the surface barrier telescopes and from the E detectors in the case of the gas-surface barrier hybrid telescopes. In the case of the gas-surface barrier telescopes, the active gas length for ΔE was 200 mm of P-10 gas maintained at a pressure of 10 mbar. At some bombarding energies, only three surface barrier ΔE-E telescopes were used. Overall normalization of the fission data was obtained using the Rutherford scattering measured by a monitor detector kept at a forward angle. Other details of the experimental set up and data analysis are the same as in our previous publication [13].

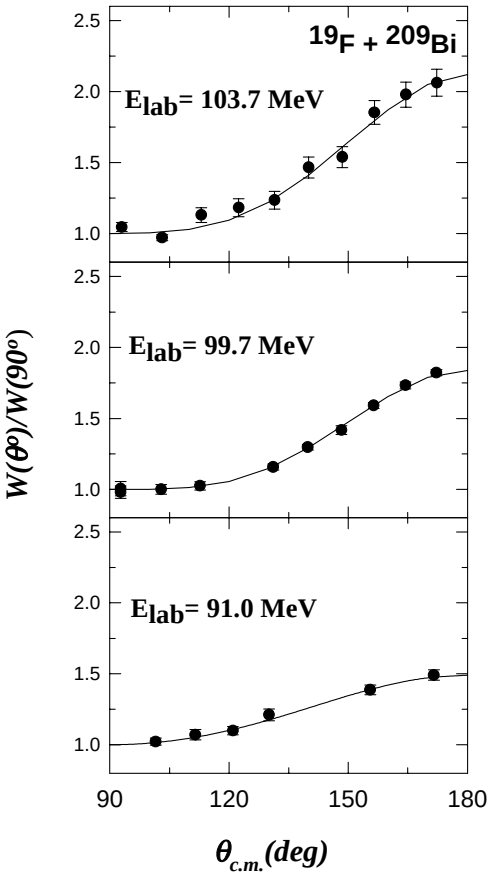

Fig. 1. Fission fragment angular distributions for the system ^{19}F + ^{209}Bi system at a few representative energies

The fission fragment angular distributions were transformed to the centre-of-mass system assuming symmetric mass division and using Viola systematics [14].

The differential fission cross sections were fitted to the sum of Legendre polynomials and are extrapolated to 180^o to obtain experimental anisotropy values. The fission fragment angular distributions measured at some energies are shown in Fig. 1 along with the fits. The total cross sections are determined by integrating the differential cross sections over all the angles. The experimental fission cross sections for various bombarding energies are listed in Table 1 along with the experimental anisotropy values. The experimental values of total fission cross sections as a function of E_{lab} for the system ^{19}F + ^{209}Bi are plotted in Fig. 2. The measured fission fragment anisotropy (A) values are plotted as a function of $E_{c.m}/V_B$ in Fig. 3. The

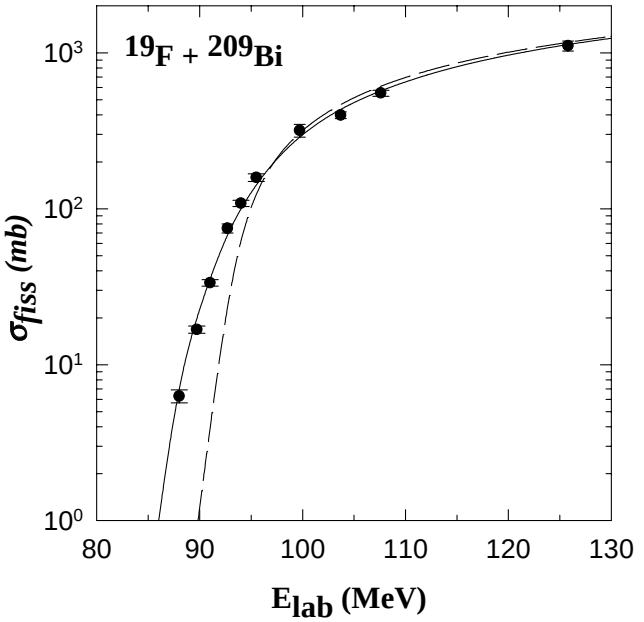

Fig. 2. Fission (Fusion) excitation function for the system ^{19}F + ^{209}Bi plotted as a function of E_{lab}. The continuous line is the coupled channels calculation. The dashed line is the calculation without the coupling

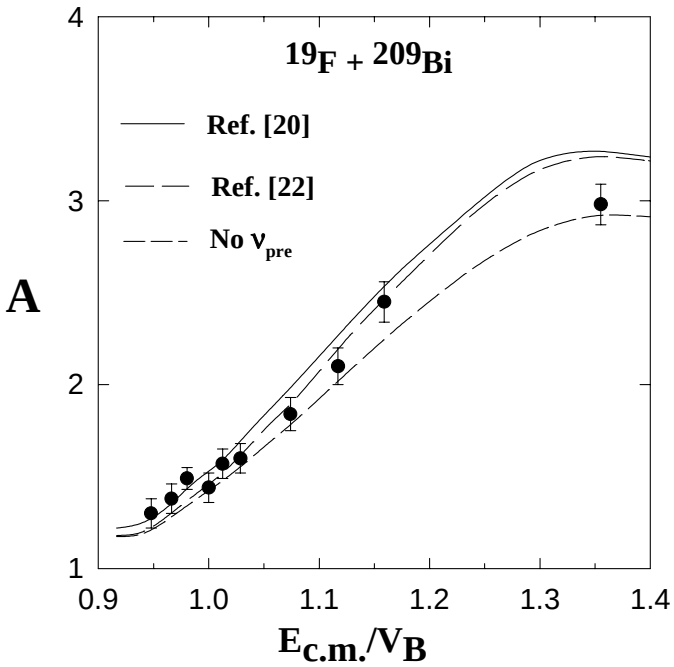

Fig. 3. The fission fragment anisotropy (A) values measured are plotted as a function of $E_{c.m.}/V_B$. The dotted, the dashed and the continuous lines are respectively the calculations with no correction for pre-fission neutrons, corrected for neutrons using the values of [22] and [20] as discussed in the text

Table 1. Fission cross sections and anisotropies for the system ^{19}F + ^{209}Bi

E_{lab} MeV	$E_{c.m.}$ MeV	$E_{c.m.}/V_B$	σ_{fiss} (mb)	Anisotropy
88.0	80.5	0.95	6.3 ± 0.6	1.30 ± 0.09
89.7	82.2	0.97	16.8 ± 1.1	1.38 ± 0.09
91.0	83.4	0.98	34.0 ± 2.0	1.49 ± 0.07
92.7	85.1	1.00	75.0 ± 5.0	1.44 ± 0.08
94.0	86.2	1.01	108.0 ± 6.0	1.57 ± 0.08
95.5	87.5	1.03	159.0 ± 9.0	1.60 ± 0.08
99.7	91.4	1.07	318.0 ± 30.0	1.84 ± 0.09
103.7	95.1	1.12	399.0 ± 20.0	2.10 ± 0.10
107.6	98.6	1.16	551.0 ± 30.0	2.45 ± 0.11
125.6	115.1	1.35	1109.0 ± 80.0	2.98 ± 0.13

errors on the fission cross sections and the anisotropies are due to counting statistics, inter-detector solid angle normalizations and fitting procedure used to extrapolate data to 180^o. The quasi-elastic (sum of elastic, inelastic and transfer channels around the elastics) angular distributions have also been measured at a bombarding energy of E = 92.7 MeV very close to the fusion barrier for this system, to deduce the corresponding fusion cross section by a procedure as discussed in [15]. The quasi-elastic angular distributions for angles beyond the Fresnel region are shown in Fig. 4. At lower angles the data have been normalised to Rutherford cross sections. From an optical model analysis of the quasi-elastic data, the fusion cross section has been determined to be 68 ± 7 mb and this compares very well with the fission cross section (75 ± 5 mb) measured at this energy. Hence it is found that the

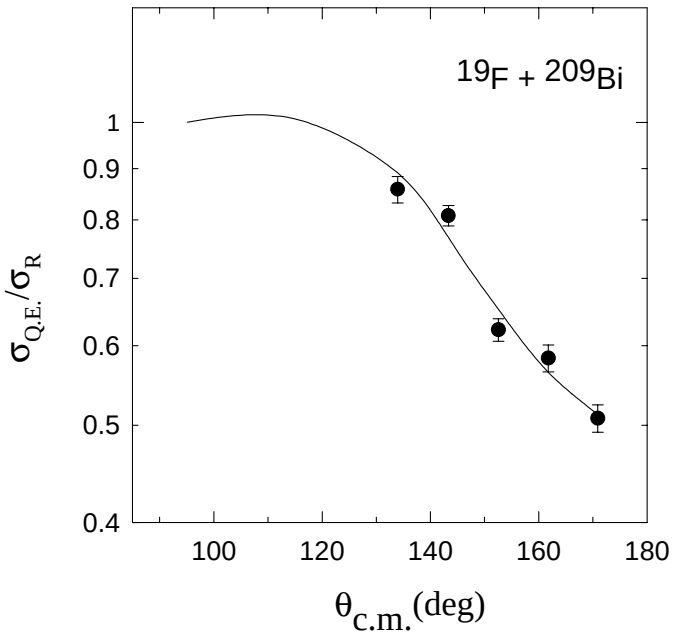

Fig. 4. Fig. 4: The quasi-elastic angular distribution plotted as a function of the scattering angle at E_{lab} = 92.7 MeV. The continuous line is the optical model fit to the data

fission cross section is the same as fusion cross section even at this low energy. Further from a statistical model analysis, it is found that it is a good assumption to treat fusion and fission cross sections to be the same for this system

over the entire energy range. This information is required in determining the spin distribution of the fissioning compound nucleus.

It has been shown in the literature that exhibiting fusion data in the form of a deduced barrier distribution is a sensitive way to bring out the underlying nuclear structure of the interacting nuclei [12]. In addition to the fission excitation function, the quasi-elastic data have been measured in the energy range from 84 to 100 MeV by employing a silicon telescope at an angle of 170^o. The extraction of the barrier distribution from this data and its implication in the determination of the angular momentum distribution of the compound nucleus is discussed in Sect. 3.1.

3 Calculation of anisotropy

The theoretical prediction of anisotropy (A) values is made on the basis of the SPSM. According to this model [16] the simplified expression for fission anisotropy is given as $A = 1 + < l^2 > /4{K_o}^2$. Here ${K_o}^2$ is the variance of the K distribuiton and $< l^2 >$ is the second moment of the compound nuclear spin distribution. ${K_o}^2$ is given as ${K_o}^2 = I_{eff}T/\hbar^2$ where I_{eff} is the effective moment of inertia and T is the temperature at the saddle. The temperature T is given as $T = \sqrt{E_x/a}$ where a is the level density parameter taken to be equal to $A_{C.N.}$ / 9 and the effective excitation energy at the saddle is given as $E_x = E_{c.m.} + Q - E_R(l) - B_f(l) - E_n$. In the above expression Q is the Q-value for compound nucleus formation, $B_f(l)$ is the l dependent fission barrier, $E_R(l)$ is the rotational energy and E_n is the energy removed by emission of neutrons (and protons) before reaching the saddle point.

3.1 Estimation of $\langle l^2 \rangle$-values

The experimental fission(fusion) excitation functions have been fitted employing the coupled channels computer code (CCDEF) [17] to obtain mean square spin values $< l^2 >$ at each energy. In the present work, we have used the following important channels: $E_x = 0.198$ MeV ($\beta_2 = 0.55$), $E_x = 1.346$ MeV ($\beta_3 = 0.33$), $E_x = 1.554$ MeV ($\beta_2 = 0.58$) and $E_x = 2.780$ MeV ($\beta_4 = 0.22$) states of ^{19}F and $E_x = 2.62$ MeV ($\beta_3 = 0.12$) and $E_x = 4.08$ MeV ($\beta_2 = 0.054$) [10] states of ^{209}Bi (taking the levels of ^{209}Bi to be the same as that of ^{208}Pb. In Fig. 2, the cross sections obtained using the coupled channel calculations (represented by the solid line) are shown. The mean square spin values at each energy have been deduced from the above calculations.

As mentioned earlier, the barrier distribution is a sensitive quantity which brings out the underlying nuclear structure of the interacting nuclei. The barrier distribution $D(B)$ can be deduced from the fusion excitation function or from the quasi-elastic excitation function as discussed in [12]. As the present fission data is not measured at closely spaced energy intervals, it has not been possible to obtain reliable $D(B)$ from the corresponding experimental data. However, the quasi-elastic data have been

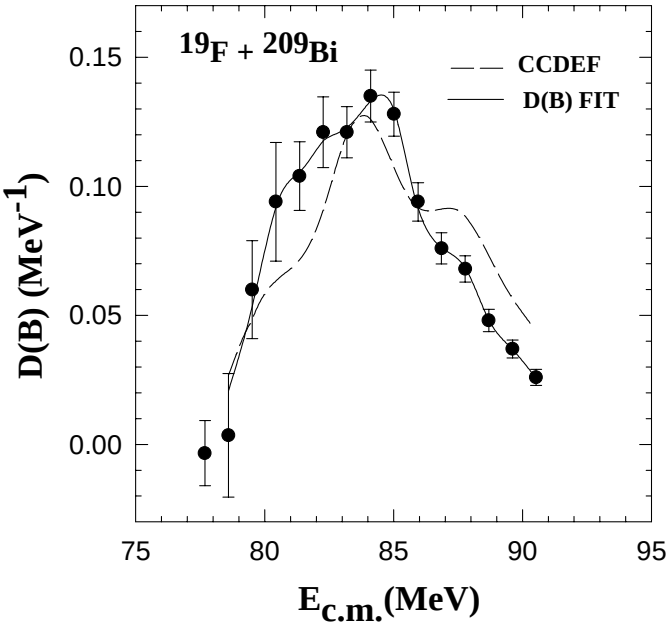

Fig. 5. The fusion barrier distribution is plotted for ^{19}F + ^{209}Bi system. The continuous line is the fit to data as per [18]. The dashed line is obtained from the fusion cross section excitation function, using CCDEF

measured at 1 MeV intervals and hence the $D(B)$ values have been deduced from this data. The same has been compared with the theoretical one obtained from the fusion excitation function calculated using CCDEF which reproduced the experimental fission data. In Fig. 5 the two barrier distributions are compared. It is found that the experimental $D(B)$ is broader than the theoretical one and the overall agreement between the two is acceptable. The barriers and their weights have also been deduced from the given barrier distribution data using the prescription of [18]. According to this model, the $D(B)$ data have been fitted using the expression-

$$D(B) = \frac{2\pi}{\hbar\omega} \sum \frac{w_i \exp(\frac{2\pi}{\hbar\omega}(E - B_i))}{[exp(\frac{2\pi}{\hbar\omega}(E - B_i)) + 1]^2} \qquad (1)$$

where w_i are the weights and B_i are the corresponding barrier heights. Only the dominant barriers have been considered. The deduced values are given in Table 2 and they compare favourably with the ones employed in fusion excitation function calculation based on nuclear strucutre of the projectile and the target as discussed earlier. Hence it is concluded that the coupling scheme used in fitting the fusion excitation data is adequate and should yield reliable values for the second moment of the spin distribution.

3.2 Estimation of ${K_o}^2$

The l dependent fission barrier ($B_f(l)$), the rotational energy ($E_R(l)$) and the effective moment of inertia ($I_{eff}(l)$) values have been taken from the prescription due to Sierk

Table 2. Fusion barrier distribution from fusion and quasi-elastic data. The columns 3 and 4 are CCDEF results

B_{QE} (MeV)	w_{QE}	B_{Fus} (MeV)	w_{Fus}
80.6 ± 0.7	0.23 ± 0.12	80.3	0.15
82.6 ± 1.1	0.24 ± 0.08	83.3	0.13
84.7 ± 0.5	0.34 ± 0.08	84.1	0.23
87.5 ± 0.5	0.17 ± 0.03	87.2	0.23
89.9 ± 0.6	0.08 ± 0.02	90.2	0.09

[19]. The values of pre-saddle neutrons which lead to cooling at the saddle-point, have been taken from the works of Rossner *et al* [20] who have determined these from actual measurements for ^{16}O + ^{208}Pb system. It has been assumed that on the average an energy of about 10 MeV is removed by every pre-saddle neutron. With these inputs, the required ${K_o}^2$ values have been calculated. Following the suggestion of Vandenbosch [21] the ${K_o}^2$ values have been corrected for the large value of the ground state spin of the target nucleus(J =9/2), using the relation $({K_o}^2)_{eff} = {K_o}^2 + J^2/3$). The fission anisotropies calculated for the present system by the above procedure are shown in Fig. 3 as a continuous line. The short-dashed curve is obtained using the pre-fission systematics from Newton [22]. The dotted line represents the calculation which does not include the neutron emission corrrection. It is found that the calculation which included the pre-saddle neutron emission provides a better description of the anisotropy data. The correction to ${K_o}^2$ due to pre-saddle neutron emission is significantly higher than that due to g.s spin of target at all the energies reported here.

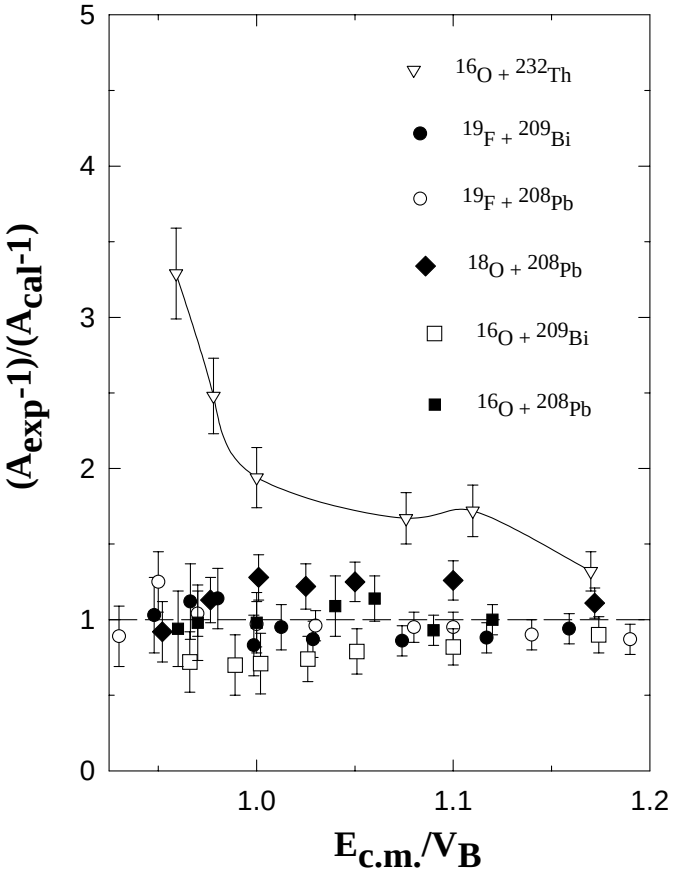

Fig. 6. The $(A_{exp}-1)/(A_{cal}-1)$ values plotted for the various systems as a function of $E_{c.m.}/V_B$

4 Discussion

It is clear from Fig. 3 that the data spanning a range of energies, $0.95 < E/V_B < 1.35$ can be adequately explained by the SPSM calculations incorporating the pre-fission neutron emission corrections. In Fig. 6, the $(A-1)_{exp}/(A-1)_{cal}$ values for several spherical systems available in the literature along with the present ones have been plotted as a function of $E_{c.m}/V_B$. It is found that by and large the values lie close to one, indicating that the anisotropies measured for the spherical target systems can be explained using the SPSM. For comparison, the values obtained for a deformed actinide target system-^{16}O + ^{232}Th- are also plotted in Fig. 6 and it clearly brings out the fact that while anomalous anisotropy values are exhibited by the deformed target system, the spherical systems show normal values. In order to investigate the role of target spin on near-barrier anisotropies in the spherical target systems, in Fig. 7, $(A-1)_{exp}/(A-1)_{cal}$ values for the ^{19}F + ^{208}Pb ($J = 0$) and ^{19}F + ^{209}Bi ($J = 9/2$) systems are plotted as a function of $E_{c.m.}/V_B$. Again the two systems have values close to one indicating that both of them are consistent with the SPSM calculations. This observation made for the spherical systems is in contrast to the one made for the deformed target systems where target spin was shown to influence the anisotropies measured [2]. It is of interest to investigate the role of B_f/T of the fissioning compound system on the measured anisotropies. For example, the PEQ fission is expected to be important for systems with low B_f/T and favourable entrance channel mass asymmetry values. As mentioned earlier, the system under investigation has the required α value. Further as the B_f / T values decrease as bombarding energy or excitation energy increases, it is expected that at the highest energy investigated, the PEQ component might be seen significantly [5], even though it might be less important at lower energies. The non-compound fission anisotropy value is expected to be energy independent and is inferred to lie between 3.5 and 5 [5,23]. At the highest energy, the compound nucleus fission anisotropy (A_{CN})is estimated to be about 3.2 from SPSM calculations. The experimental value is 2.98 ± 0.13 and this is somewhat lower than the A_{CN}. This being the case it is concluded that the PEQ component is negligible even at this energy. Measurements are required at still higher energies to improve the sensitivity of estimation of PEQ component.

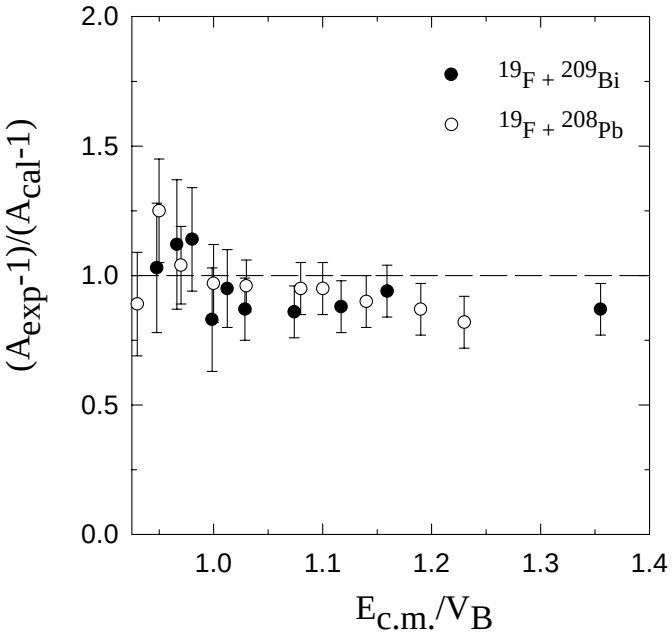

Fig. 7. The same quantity as in Fig. 6 plotted separately for $^{19}F + ^{208}Pb$ and ^{209}Bi systems

5 Summary

The fission fragment angular distributions have been reported for the system $^{19}F + ^{209}Bi$ in the energy range 88 to 125.6 MeV. The fission cross sections are described well using the coupled channels reaction model which included the prominent excitations of the projectile and the target. The SPSM calculations which incorporated corrections for pre-saddle neutron emission are able to reproduce the measured fission anisotropy data over the entire energy region from near to well above the fusion barrier. Combining this result with the literature data for other projectiles interacting with Pb/Bi targets, it is concluded that the spherical targets display nearly normal anisotropies at near and above barrier energies. From the measured fission anisotropy data and an improved SPSM analysis, the PEQ fission component is estimated to be negligible even at the highest energy investigated where the B_f/T value is relatively more favourable for occurrence of this non-equilibrium fission process.

The authors would like to thank the Pelletron operating staff for the efficient operation of the machine during the experiment. Thanks are also due to Drs. S. K. Datta, M. Sharan, S. Mandal and Mr. T. Madhusoodhanan for their help in data collection and the operating staff of the Delhi pelletron for the smooth operation of the machine during the experiment.

References

1. S. Kailas, Phys. Rep. **284**, 381 (1997); J. Phys. G. Nucl.Phys. **23**, 1227 (1997)
2. J. P. Lestone, A. A. Sonzogni, M. P. Kelly and R. Vandenbosch, Phys. Rev. **C56**, 2907 (1997)
3. R. Vandenbosch, J. D. Bierman, J. P. Lestone, J. F. Liang, D. J. Prindle, A. A. Sonzogni, S. Kailas, D. M. Nadkarni, S. S. Kapoor, Phys. Rev. **C54**, R977 (1996); S. Kailas, D. M. Nadkarni, A. Chatterjee, A. Saxena, S. S. Kapoor, R. Vandenbosch, J. P. Lestone, J. F. Liang, D. J. Prindle, A. A. Sonzogni, J. D. Bierman, Phys. Rev. **C59**, 2580 (1999)
4. A. Shrivastava, S. Kailas, A. Chatterjee, A. M. Samant, A. Navin, P. Singh, B. S. Tomar, Phys. Rev. Lett. **82**, 699 (1999)
5. V. S. Ramamurthy and S. S. Kapoor, Phys. Rev. Lett. **54**, 178 (1985); V. S. Ramamurthy, S. S. Kapoor, R. K. Choudhury, A. Saxena, D. M. Nadkarni, A. K. Mohanty, B. K. Nayak, S. V. Sastry, S. Kailas, A. Chatterjee, P. Singh and A. Navin, Phys. Rev. Lett. **65**, 25 (1990)
6. A. M. Samant and S. Kailas, Z. Phys. **A356**, 309 (1996)
7. E. Vulgaris, L. Grodgins, S. G. Steadman and R. Ledoux, Phys. Rev. **C33**, 2017 (1986); S. Kailas and P. Singh, Z. Phys. **A347**, 267 (1994)
8. C. R. Morton, D. J. Hinde, J. R. Leigh, J. P. Lestone, M. Dasgupta, J. C. Mein, J. O. Newton and H. Timmers, Phys. Rev. **C52**, 243 (1995)
9. G. Ravi Prasad, A. M. Samant, A. Shrivastava, A. Navin, A. Chatterjee, P. Singh, S. Kailas and V. S. Ramamurthy, Phys. Rev. **C57**, 971 (1998)
10. H. Zhang, Z. Liu, J. Xu, K. Xu, J. Lu and M. Ruan, Nucl. Phys. **A512**, 531 (1990)
11. B. B. Back, R. R. Betts, J. E. Gindler, B. D. Wilkins, S. S. Saini, M. B. Tsang, C. K. Gelbke, W. G. Lynch, M. A. McMahan and P. A. Baisden, Phys. Rev. **C32**, 195 (1985)
12. D. J. Hinde and M. Dasgupta, Australian National University report (ANU-P/1340(1997)) and (ANU-P/1381(1998); M. Dasgupta, D.J.Hinde, N.Rowley and A.M.Stefanini, Ann. Rev. Nuclear and Particle Science.**48**,401 (1998)
13. A. Karnik, S. Kailas, A. Chatterjee, A. Navin, A. Shrivastava, P. Singh and M. S. Samant Phys. Rev. **C52**, 3189 (1995)
14. V. E. Viola, K. Kwiatkowski and M. Walker, Phys. Rev. **C31**, 1550 (1985)
15. A. Shrivastava, S. Kailas, P. Singh, A. Chatterjee, A. Navin, A. M. Samant, V. Ramdev Raj, S. Mandal, S. K. Datta, D. K. Awasthi, Nucl. Phys. **A635**, 411 (1998)
16. I. Halpern and V. M. Strutinsky, Proc. Int. Conf. Peaceful uses of Atomic Energy, Geneva, vol. **15**, 408 (1958); R. Vandenbosch and J. R. Huizenga, Nuclear fission, (Academic press, New York,1973)
17. J. Fernandez-Niello, C. H. Dasso and S. Landowne, Com. Phys. Comm. **54**, 409 (1989)
18. H. Timmers, D. Ackermann, S. Beghini, L. Corradi, J. H. He, G. Montagnoli, F. Scarlassara, A. M. Stefanini, N. Rowley, Nucl. Phys. **A 633**, 421 (1998)
19. A. J. Sierk Phys. Rev. **C33**, 2039 (1986)
20. H. Rossner, D. J. Hinde, J. R. Leigh, J. P. Lestone, J. O. Newton, J. X. Wei and S. Elfstrom, Phys. Rev. **C45**, 719 (1992)
21. R. Vandenbosch (private communication); S. Kailas and P. Singh, Z. Phys. **A347**, 267 (1994)
22. J. O. Newton, Sov. J. Nucl. Phys.**21**, 349 (1990)
23. D. Vorkapic and B. Ivanisevic, Phys. Rev. **C52**, 1980 (1995)